High-ρR Implosions for Fast-Ignition Fuel Assembly

C. D. Zhou,[1,2] W. Theobald,[1] R. Betti,[2] P. B. Radha,[1] V. A. Smalyuk,[1] D. Shvarts,[3] V. Yu. Glebov,[1] C. Stoeckl,[1] K. S. Anderson,[1] D. D. Meyerhofer,[1,2] and T. C. Sangster[1]

[1]*Fusion Science Center and Laboratory for Laser Energetics, University of Rochester, New York 14623, USA*
[2]*Dept. of Mechanical Eng. & Physics and Astronomy, University of Rochester, Rochester, New York 14627, USA*
[3]*NRCN, Negev and Ben Gurion University of the Negev, Beer-Sheva 84015, Israel*

C. K. Li, R. D. Petrasso, J. A. Frenje, and F. H. Seguin

MIT Plasma Science and Fusion Center & Fusion Science Center, Cambridge Massachusetts, 02139, USA
(Received 28 October 2006; published 11 January 2007)

Thick, 40 μm plastic shells filled with 25–35 atm of D_2 or D^3He were imploded on a low-adiabat ($\alpha \approx 1.3$) and with a low-implosion velocity ($\sim 2 \times 10^7$ cm/s) on the OMEGA laser to generate massive cores of compressed plasma with high areal densities optimal for fast ignition. The targets are driven by 20-kJ relaxation adiabat-shaping laser pulses to keep the inner portion of the shell nearly Fermi degenerate. The measured kinetic energy downshift of proton spectra is in good agreement with the theoretical predictions yielding burn-averaged areal densities of 0.130 ± 0.017 g/cm^2 and peak ρR during the burn of about 0.24 ± 0.018 g/cm^2, the largest ρR measured on OMEGA to date. The same implosions with empty plastic shells are expected to reach 1.3 g/cm^2 across the core (i.e., $2\rho R$) enough to stop fast electrons with energies up to 4.5 MeV typical of fast ignition scenarios.

DOI: 10.1103/PhysRevLett.98.025004 PACS numbers: 52.57.Kk

In direct-drive [1] and fast-ignition inertial confinement fusion [2], a cryogenic shell of deuterium and tritium (DT) filled with DT gas is accelerated inward by direct laser irradiation (direct-drive). If the thermonuclear fuel is ignited and a burn wave propagates through the dense core, the fusion energy produced can greatly exceed the laser energy used to drive the target. The energy gain G is defined as the ratio between the thermonuclear energy yield and the laser energy on target. As shown in Ref. [3], the gain is directly related to the capsule implosion velocity and the areal density through the simple relation

$$G \approx \frac{73}{I_{15}^{0.25}} \left(\frac{3 \times 10^7}{V_I}\right)^{1.25} \frac{\theta(\rho R)}{0.2} \tag{1}$$

where V_I is in cm/s. The function θ represents the fraction of burned fuel depending on the fuel areal density $\rho R \equiv \int_0^\infty \rho dr$. The function $\theta = \theta(\rho R)$ is commonly approximated [1] by $\theta \simeq (1 + 7/\rho R)^{-1}$, where ρR is given in g/cm^2. A simple expression for the peak areal density of DT capsules with 1 atm gas fill is derived in Ref. [3], yielding a scaling independent of velocity,

$$\rho R_{\max} \approx \frac{1.2}{\alpha_{\text{inn}}^{0.55}} \left(\frac{E_L(kJ)}{100}\right)^{0.33} \tag{2}$$

where α_{inn} is the adiabat of the inner portion of the shell and ρR is in g/cm^2. In implosion hydrodynamics, the adiabat is usually referred to as the ratio of the pressure to the Fermi pressure of a fully degenerate electron gas. The adiabat is a measure of the entropy and is typically set by the shocks propagating through the target. The inner adiabat determines the areal density because the outer portion of the shell is ablated during the implosion and only the inner portion is left to form the dense stagnating core. For a given laser energy, higher areal densities require lower inner adiabats, and higher gains can be achieved through lower implosion velocities (and greater fuel mass) and lower adiabats. A low-implosion velocity also leads to a small, cold and dense hot spot [3] and to a fuel assembly close to a uniform density core.

Based on these results, it was concluded in Ref. [3] that using slow, low-adiabat implosions of massive shells is a viable approach to generate a high areal density assembly for fast-ignition. This approach should also improve the performance of cone-in-shell targets where a gold cone is inserted into the shell to keep a plasma-free path for the fast ignitor pulse [4]. Recent experiments and simulations of cone-in-shell target implosions [5] have shown that the integrity of the cone tip is compromised by the large hydrodynamic pressures and that a low density plasma region develops between the cone tip and the dense core, thus complicating the fast electron transport. The fuel assemblies studied in this Letter can improve the cone target performances since the resulting dense core has relatively low pressure (due to the low velocity) and large size (due to the massive shells), thus reducing the hydrodynamic forces on the cone tip and the distance between the tip and the dense core edge. The use of adiabat-shaping pulses to perform fast-ignition implosions was suggested in Ref. [3]. The relaxation technique [6] for adiabat shaping simplifies the laser pulse by lowering the contrast ratio between the peak laser power and the power in the foot of the main pulse. It also improves the hydrodynamic stability of the implosion by decreasing the in-flight aspect ratio and by increasing the ablation velocity.

This Letter reports experimental results of implosions carried out at the OMEGA laser facility that were designed

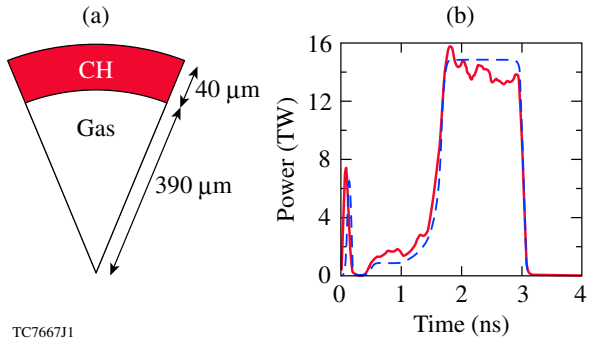

FIG. 1 (color online). (a) Plastic capsule is filled with D_2 or D^3He used on OMEGA. (b) Designed (dashed line) and measured (solid line) pulse shapes for shot 43075.

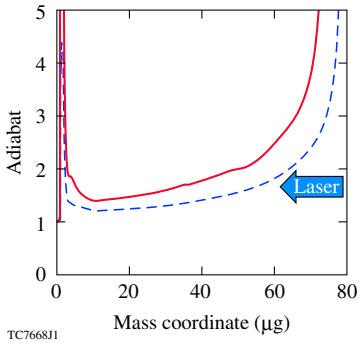

FIG. 2 (color online). Simulated adiabat profile versus mass coordinate at shock breakout for the designed (dashed line) and the measured (solid line) from pulse shapes.

to achieve high areal densities according to the theory outlined in Ref. [3]. The targets were massive 40 μm thick, 430 μm in outer radius, plastic shells coated outside with a 0.1 μm layer of aluminum. The capsules, shown in Fig. 1(a) are filled with either D_2 or D^3He gas with various pressures ranging from 25 to 34 atm. The capsules were imploded by a ~20-kJ UV laser pulse. The 351-nm wavelength laser light was smoothed with distributed polarization rotators [7] and distributed phase plates. Figure 1(b) shows the laser pulse shape that is based on the relaxation technique. It consists of an 80 ps FWHM Gaussian prepulse, followed by a 300 ps long laser shut-off, and the main laser pulse with a foot power of about 1 TW and a peak power of about 14 TW. The main laser pulse contrast ratio (peak power/foot power) is about 14 and well within the OMEGA contrast ratio capabilities. This laser pulse generates a shaped adiabat profile within the shell that is monotonically decreasing from the outer (ablation) surface toward the inner shell surface. The laser pulse design, represented by the dashed line, is compared with the measured experimental pulse (solid line) for laser shot 43075 [Fig. 1(b)]. According to one dimensional hydrodynamic simulations carried out with the code LILAC [8], the adiabat at main-shock breakout at the inner surface is nearly Fermi degenerate $\alpha_{\text{inn}} \approx 1.3$. These are likely the lowest adiabat direct-drive implosions carried out to date. Figure 2 compares the simulated adiabat profiles at shock breakout versus the mass coordinate (measured from the center of the capsule) of the designed pulse shape (dashed line) and the measured pulse shape (solid line) taken from Fig. 1(b). The implosion velocity inferred from the simulations reaches the peak values of 2×10^7 cm/s at about 3.4 ns.

The kinetic energy downshift of protons generated by the $D + {}^3$He fusion reactions, which is the primary reaction in D^3He-fuel and a secondary reaction in D_2-fuel, was used to infer the areal density [9]. The primary reaction in D^3He generates monoenergetic 14.7 MeV protons, and the secondary reaction in D_2 yields 12.6 to 17.5 MeV protons due to the kinetic energy spread of ^{3}He. The proton spectrum was measured with wedge-range-filters (WRF) [10,11] at various locations around the target. Two kinds of WRF's were used. The first covers the spectral range down to ~8 MeV, and the second, using thinner wedges, measures down to ~3 MeV kinetic energy. Areal density measurements based on the fusion proton spectrum downshift are routinely used by the Rochester [11,12] and Osaka [13] groups, in addition to other nuclear diagnostics [14].

Spectra were measured from 5 different directions. Figure 3 shows the measured proton spectrum summed over all directions for a 25 atm D_2-fill implosion for laser shot 43075 (solid) with a pulse energy of 20.5 kJ. An average downshift of 4.1 ± 0.3 MeV was measured. The absolute calibration uncertainty of the WRF is ±0.4 MeV for the mean value of the proton spectral distribution. Following Ref. [9], an areal density averaged over the duration of proton production of $\langle \rho R \rangle = 0.146 \pm 0.009$ g/cm^2 is inferred from the spectrum (solid) in Fig. 3 assuming burn-averaged density of 115 g/cm^3 and a plasma temperature of 0.1 keV, taken from the simulations. The peak density of about 200 g/cm^3 occurs at the end of the fusion burn. There is a slight dependency of the inferred ρR-value on the density. A density variation of ±50 g/cm^3 changes the areal density by ~ ± 0.010 g/cm^2. The temperature dependence is negligible. Taking the statistical fluctuation, the density variation, and the calibration uncertainty into account, a measurement error of ~ ± 0.017 g/cm^2 is esti-

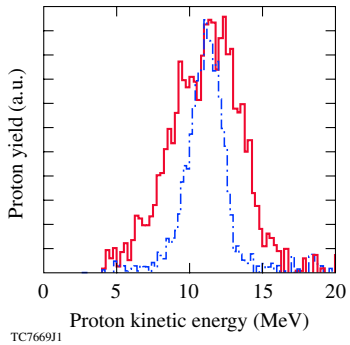

FIG. 3 (color online). Measured proton spectra for shot 43075 (solid line) and shots 43110 plus 43113 (dashed-dotted line).

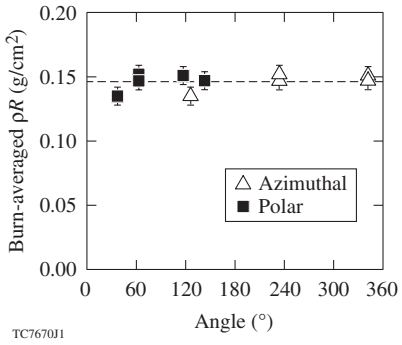

FIG. 4. Measured burn-averaged areal density in 5 directions for shot 43075 (25 atm D_2, 20.5-kJ laser energy). The open triangles show ρR versus the azimuthal coordinate, and the solid squares are versus the polar coordinate.

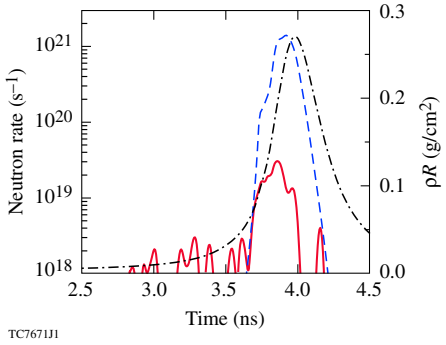

FIG. 5 (color online). Predicted neutron rate (dashed line), calculated areal density history (dashed-dotted line), and the measured neutron rate (solid line) for shot 43075. Truncation of the burn at peak compression allows to sample only early in the areal density evolution.

mated for the inferred areal density. Figure 4 shows the experimentally-inferred burn-averaged areal density for shot 43075 in various directions. The ρR-modulations are quite small ($<10\%$) and are comparable to the statistical uncertainty of the measurement, indicating that the compressed core is not significantly affected by low mode ($\ell \lesssim 5$) nonuniformities [15]. Figure 3 also shows the spectrum from 25 atm D^3He-fill implosions (dashed-dotted line). The proton yield of two laser shots (43110 with 20.2 kJ and 43113 with 20.8 kJ) under the same experimental conditions was summed to improve the statistics. An energy shift of 3.86 MeV corresponding to $\langle \rho R \rangle = 0.130 \pm 0.008$ g/cm^2 is obtained. A narrower spectral distribution is measured due to the monoenergetic birth proton energy. The standard deviation of $\langle \rho R \rangle$ from the different directions is less than 10%. For shot 43075, a total proton yield of $(1.23 \pm 0.47) \times 10^7$ and for 43110 plus 43113 $(0.75 \pm 0.21) \times 10^7$ were measured, which is $\sim$1 to 3% of the proton yield predicted by the 1D-simulations. This is similar to the neutron over clean yields that are also in the few percent range. Such low yields over clean are likely due to the shell-fuel mix [16] induced by the large convergence ratio of the fuel (16 for 25 atm, 21 for 15 atm) and the slow assembly, and are consistent with a clean hot spot radius equal to the so-called free fall line [17]. The fuel-shell mix causes a lower and truncated fusion rate as shown in Fig. 5 where the solid line is the measured neutron rate and the dashed line is the simulated one. Mixing is enhanced in these low velocity FI implosions because the hot spot is small relative to the target size [3]. Indications that small scale length mixing is important were also found experimentally by the increase of the yield over clean by a factor of $\sim$3 by reducing convergence with increasing fill pressure from 13 to 34 atm.

The proton spectrum verifies the predicted $\rho R(t)$ evolution during the burn. Notice that each point of the proton energy spectrum (Fig. 3) corresponds to a different downshift and therefore to a different ρR. The simulations indicate that ρR (Fig. 5) increases during the burn and that the burn is quenched near the time of peak areal density. Thus, the energy downshift of the low energy tail of the spectrum represents a measure of the peak ρR during the burn approximately equal to the simulated peak ρR. This is verified by reconstructing the proton spectrum using the simulated $\rho R(t)$ evolution (dashed-dotted line in Fig. 5) and the experimental neutron rate (solid line). The temporal shape of the neutron rate is close to the secondary proton rate and can be used to reconstruct the proton spectrum. Using the measured neutron rate is justified since the rise of the simulated and measured neutron rates is closely matched. At each time, the proton energy is downshifted according to the simulated ρR and the energy loss formula of Ref. [18]. The resulting proton spectrum is compared with the measured one in Fig. 6. The broadening effect [12] due to the finite source size of the secondary protons is included. The dashed line in Fig. 6 is the reconstructed spectrum including the source broadening effect for a source size as predicted by the 1D simulations. The dashed-dotted line is for a point source. Since the measured fusion yield is significantly lower than 1D predictions, the effect of fuel-shell mixing is expected to reduce the hot spot size. Thus, we expect the finite source

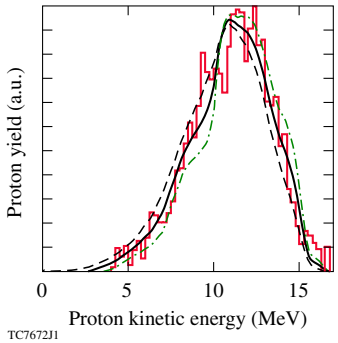

FIG. 6 (color online). Measured proton spectrum (solid line) compared to the predicted spectrum using 1D simulations and measured neutron rates for shot 43075. The dashed line is for the extended 1D source, the dashed-dotted line is for a point source and the solid line is the average of the two.

TABLE I. Measured and simulated areal densities in g/cm^2 for different fills and gas pressures (in atm). The laser energy in shot 43114 was only 16 kJ.

Shot Number	Gas fill	Pressure	Measured $\langle \rho R \rangle_p$	Sim. shell $\langle \rho R \rangle_n$	Measured $\rho R^{\max}$	Sim. $\rho R^{\max}$
43074	D_2	34	0.133	0.138	0.249	0.238
43075	D_2	25	0.146	0.144	0.261	0.261
43107	D_2	25	0.122	0.132	0.240	0.275
43114	D_2	25	0.128	0.112	0.227	0.227
43109 + 43112	D^3He	33	0.128	-	0.24	0.250
43110 + 43113	D^3He	25	0.130	-	0.24	0.281
average			0.131	0.132	0.243	0.255

size effect to produce a spectrum broadening of a magnitude intermediate between the point source and the 1D source. The solid line represents the arithmetic average of the dashed-dotted and dashed lines. The good agreement between the measured spectrum and the reconstructed spectrum indicates that the simulated $\rho R(t)$ evolution is fully consistent with the measured spectrum during the burn. Such a good agreement provides the needed confidence to infer the maximum ρR from the maximum downshift of the spectrum, leading to a peak ρR of 0.261 g/cm^2.

Table I shows the burn-averaged ρR as well as the maximum ρR during burn from the tail of the proton spectrum for several shots. The measured neutron yields of the D_2 targets with a fill pressure of 25–34 atm were in the range of 2–4 $\times$ 10^9, large enough to generate a measurable neutron rate well above the noise level allowing the computation of the neutron averaged ρR and the spectrum reconstruction from the 1D hydro code (Fig. 6). The burn-average is a time averaged value over the proton production rate and has been compared with the simulated ρR averaged over the experimentally measured neutron rate (solid line in Fig. 5) from the $D + D$ fusion reactions. Averaging the simulated ρR over the proton rate was not possible for D^3He-filled capsules, since no useful neutron rates were measured due to the low yields of the $D + {}^3$He reactions. However, because of the clean and narrow spectrum of the primary protons, a fairly accurate estimate of the energy tail can be inferred for the D^3He fills even in the absence of the spectrum reconstruction. Figure 3 shows an energy tail of about 7 MeV for the primary spectrum (dashed-dotted line) corresponding to a peak areal density of 0.24 g/cm^2.

In conclusion, the measured areal densities are in very good agreement with the neutron averaged and peak ρR from the 1D simulations of the D_2 capsules for 25 and 33 atm fill pressures where the measured neutron rate is used to reconstruct the proton spectrum from the simulated $\rho R(t)$ evolution. The mean value of the measured burn-averaged ρR over all shots is 0.130 ± 0.017 g/cm^2 and agrees well with the mean theoretical value of 0.132 g/cm^2. The peak ρR measured from the tail of the spectrum and averaged over all shots is 0.240 ± 0.018 g/cm^2. It compares favorably with the simulated value of 0.25 g/cm^2. Such ρRs are the largest areal densities assembled on OMEGA to date. The peak ρR across the entire core (i.e., $2\rho R$) is about 0.5 g/cm^2 sufficient to slow down 2 MeV electrons. For equivalent fast-ignition empty CH capsules, 1D simulations indicate a maximum $\rho R \approx 0.66$ g/cm^2, or an areal density about 1.3 g/cm^2 through the entire core enough to stop 4.5 MeV electrons. Such dense cores are optimal for studying fast electron coupling efficiencies in integrated fast-ignition experiments. These results show that low velocity, low-adiabat implosions are a viable approach of assembling high areal density fuel for fast ignition. Equivalent cryogenic implosions on OMEGA are expected to achieve $\rho R \sim 0.6$ g/cm^2 [Eq. (2)] and density of 350 g/cm^3.

This work has been supported by the US Department of Energy under Cooperative Agreement No. DE-FC02-04ER54789 (Fusion Science Center) and No. DE-FC03-92SF19460 (Office of Inertial Confinement Fusion).

[1] S. Atzeni and J. Meyer-ter-Vehn, *The Physics of Inertial Fusion* (Clarendon, Oxford, 2004).
[2] M. Tabak *et al.*, Phys. Plasmas **1**, 1626 (1994); S. Atzeni, Phys. Plasmas **6**, 3316 (1999).
[3] R. Betti and C. Zhou, Phys. Plasmas **12**, 110702 (2005).
[4] R. Kodama *et al.*, Nature (London) **412**, 798 (2001); K. A. Tanaka *et al.*, Phys. Plasmas **10**, 1925 (2003); P. Norreys *et al.*, Phys. Plasmas **11**, 2746 (2004).
[5] R. Stephens *et al.*, Phys. Plasmas **12**, 056312 (2005).
[6] K. Anderson and R. Betti, Phys. Plasmas **11**, 5 (2004).
[7] T. R. Boehly *et al.*, J. Appl. Phys. **85**, 3444 (1999).
[8] M. C. Richardson *et al.*, *Laser Interaction and Related Plasma Phenomena* (Plenum, New York, 1986) Vol. 7, p. 421.
[9] C. K. Li *et al.*, Phys. Plasmas **7**, 2578 (2000).
[10] F. H. Seguin *et al.*, Rev. Sci. Instrum. **74**, 975 (2003).
[11] R. D. Petrasso *et al.*, Phys. Rev. Lett. **90**, 095002 (2003).
[12] V. A. Smalyuk *et al.*, Phys. Rev. Lett. **90**, 135002 (2003).
[13] Y. Kitagawa *et al.*, Phys. Rev. Lett. **75**, 3130 (1995).
[14] H. Azechi *et al.*, Laser Part. Beams **9**, 193 (1991).
[15] C. K. Li *et al.*, Phys. Rev. Lett. **92**, 205001 (2004).
[16] P. B. Radha *et al.*, Phys. Plasmas **12**, 056307 (2005).
[17] P. D. Roberts *et al.*, J. Phys. D **13**, 1957 (1980).
[18] C. K. Li and R. D. Petrasso, Phys. Rev. Lett. **70**, 3059 (1993).